1   **Using mercury isotopes to understand the bioaccumulation of Hg in the subtropical Pearl**

2   **River Estuary, South China**

3

4   Runsheng Yin [a, b], Xinbin Feng [c], Junjun Zhang [a], Ke Pan [d], Wenxiong Wang [d], Xiangdong Li [a, *]

5

6   [a] Department of Civil and Environmental Engineering, The Hong Kong Polytechnic University,

7   Hung Hom, Kowloon, Hong Kong

8   [b] State Key Laboratory of Ore Deposit Geochemistry, Institute of Geochemistry, Chinese

9   Academy of Sciences, Guiyang 550002, China

10   [c] State Key Laboratory of Environmental Geochemistry, Institute of Geochemistry, Chinese

11   Academy of Sciences, Guiyang 550002, China

12   [d] Division of Life Science, The Hong Kong University of Science and Technology, Clearwater

13   Bay, Kowloon, Hong Kong

14

15   * Corresponding author

16   E-mail address: cexdli@polyu.edu.hk (X. Li).

17

18

19

ABSTRACT

Coastal and estuarine regions are important areas of mercury pollution. Therefore, it is important to properly characterize the sources and bioaccumulation processes of mercury in these regions. Here, we present mercury stable isotopic compositions in 18 species of wild marine fish collected from the Pearl River Estuary (PRE), south China. Our results showed variations in mass-independent fractionation (Δ^{199}Hg: $+0.05 \pm 0.10$‰ to $+0.59 \pm 0.30$‰) with a Δ^{199}Hg / Δ^{201}Hg of ~1.26, suggesting that aqueous MeHg underwent photo-degradation prior to incorporation into the food chain. For the results, we discovered small but significant differences of Δ^{199}Hg values among herbivorous, demersal, and carnivorous fish, indicating that different feeding guilds of fish may have incorporated MeHg with various degrees of photo-demethylation. The consistent mercury isotope compositions between fish feeding habitat and mercury sources in the estuary provide potentially important findings on the transformation and bioaccumulation of this toxic metal in subtropical coastal environments.

INTRODUCTION

Mercury (Hg), a global pollutant, is released into the environ- ment from both natural and anthropogenic sources. In an aqueous environment, inorganic Hg (IHg) can form methyl mercury (MeHg), a more toxic form that is readily bioaccumulated and biomagnified in aquatic food chains, posing a significant threat to aquatic eco- systems and human health (Fitzgerald et al., 2007; Blum et al., 2013). Anthropogenic activities have greatly altered the sources and biogeochemical processes of Hg, however, its impact on the transformation and bioaccumulation in the aqueous environment is less clear (Fitzgerald et al., 2007).

With the recent documentation showing that Hg isotopes exhibit mass-dependent fractionation (MDF, as δ^{202}Hg values) and mass-independent fractionation (MIF, as Δ^{199}Hg values), Hg isotope geochemistry has greatly increased our understanding of the sources and fates of this toxin (Hintelmann, 2012; Blum et al., 2014; Yin et al., 2010a, 2014). Similar to δ^{13}C and δ^{15}N, Hg isotopes may offer insights into the sources and biogeochemical behavior of Hg in food webs (Bergquist and Blum, 2007; Senn et al., 2010; Jackson et al., 2008; Das et al., 2009; Gantner et al., 2009; Laffont et al., 2009, 2011; Gehrke et al., 2011; Perrot et al., 2010, 2012; Kwon

et al., 2012, 2013, 2014; Blum et al., 2013; Li et al., 2014).

The δ^{202}Hg values have been applied to link fish and Hg sources. For instance, a strong correlation between d202Hg in fish and that in co-located intertidal sediments was found in the San Francisco Estuary, USA (Gehrke et al., 2011). However, the use of fish δ^{202}Hg to trace Hg sources was called into question by the occurrence of Hg- MDF during Hg bioaccumulation (Jackson et al., 2008; Das et al., 2009). Higher δ^{202}Hg values have been observed in mammal predators [e.g., humans (Laffont et al., 2009, 2011; Sherman et al., 2013), whales (Li et al., 2014), seals (Perrot et al., 2012), and birds (Point et al., 2011)] than in their fish prey. Recent studies observed no Hg-MDF during MeHg bioaccumulation by fish (Kwon et al., 2012, 2013), whereas intestinal MeHg degradation can cause significant MDF in mammals (Sherman et al., 2013). The most intriguing finding is the observation of Hg-MIF in fish (Bergquist and Blum, 2007; Jackson et al., 2008; Das et al., 2009; Gantner et al., 2009; Laffont et al., 2009, 2011; Gehrke et al., 2011; Perrot et al., 2010, 2012; Senn et al., 2010; Kwon et al., 2012, 2013, 2014; Blum et al., 2013; Li et al., 2014). The Hg-MIF in fish was initially explained to be caused during in vivo biological processes (Das et al., 2009), whereas such an explanation is not supported by the observation of no Hg-MIF during microbial transformations (Rodríguez-Gonza,lez et al., 2009; Kritee et al., 2013; Jime,nez-

65 Moreno et al., 2013), bioaccumulation and trophic transfer (Laffont et al., 2009, 2011; Perrot et

66 al., 2012; Kwon et al., 2012, 2013; Blum et al., 2013). The Hg-MIF in fish was later explained by

67 the aqueous MeHg photo-degradation process prior to bio- accumulation, due to the fact that >90%

68 of Hg in fish is MeHg (Blum et al., 2013). With unperturbed Hg-MIF during bioaccumulation, it

69 is speculated that fish Hg-MIF can provide important information on the photochemical cycling of

70 MeHg in aquatic ecosystems (Bergquist and Blum, 2007; Blum et al., 2013). For instance, higher

71 Hg-MIF (Δ^{199}Hg > 1‰) has been documented in pelagic fish than in coastal fish (Δ^{199}Hg < 1‰),

72 indicating that MeHg in the open ocean water column is subjected to more photo-degradation than

73 in coastal waters (Gehrke et al., 2011; Senn et al., 2010; Blum et al., 2013; Kwon et al., 2014). A

74 systematic decline in Δ^{199}Hg values with the depth of fish feed was observed, suggesting that Hg-

75 MIF can be a good indicator of the feeding depth of fish (Blum et al., 2013).

76 The Pearl River Estuary (PRE) is a subtropical estuary located in the northern part of the South

77 China Sea (SCS) (Fig. 1). During the last few decades, rapid economic development in the

78 surrounding Pearl River Delta (PRD) region has led to excessive discharges of Hg and other

79 pollutants into the PRE (Fu et al., 2010; Liu et al., 2011, 2012). Our recent study investigated Hg

80 isotopes in surface sediments of the PRE, which indicated that the PRE receives Hg from

81 atmospheric deposition, industrial waste discharges, urban emissions, and watershed runoff, with

82 distinct Hg isotopic signatures (Yin et al., 2015). However, the impact of Hg pollution on the bio-

83 accumulation in the aquatic food web in such a subtropical region is poorly understood. Here, we

84 investigated the Hg isotopic variations in 18 fish species in the PRE. The objectives of this study

85 were (1) to investigate the sources of MeHg in different feeding guilds of fish; (2) to evaluate the

86 capability of Hg isotopes in tracking Hg through aquatic food webs using Hg isotopes; and (3) to

87 evaluate the potential effect of human activities on Hg dynamics in food webs of the PRE.

MATERIALS AND METHODS

Fish Sampling

The PRE (Fig. 1) covers an area of ~2000 km^2, with depths varying from 0 to 30 m. The average distance is 49 km from north to south, and 4—58 km from east to west (Shi et al., 2010; Yin et al., 2015). A total of 39 individual fish from 18 species of fish were collected in the PRE from August to December 2011. Details of the processing of the samples, the total mercury (THg) concentrations (9.5 ± 2.4 to 53 ± 15.2 ng g^{-1} wet weight), the MeHg concentrations (8.4 ± 1.9 to 50.3 ± 16.0 ng g^{-1} wet weight), the $\delta^{15}N$ (10.2 ± 0.4‰ to 18.7 ± 0.4‰), and the $\delta^{13}N$ (—23.4 ± 0.5‰ to 16.9 ± 0.2‰) of the fish samples have been given by Pan et al. (2014). The average fraction of MeHg (F_{MeHg}) in the fish ranged from 87.6 ± 4.8% to 102.5 ± 7.8%, consistent with the previous finding that the majority of the Hg in fish was MeHg (Fitzgerald et al., 2007; Blum et al., 2013). The analyses of Hg isotopes performed in this study were for THg. Based on THg, $\delta^{15}N$ data, and dietary information, the fish in the PRE can be categorized into three main groups: herbivorous, demersal, and carnivorous (Fig. 2).

Hg isotopic composition analysis

About 0.5 g of dried samples (wet/dry ratio: 4.2—4.5) were weighed and digested at 95°C for 3 h with a 10 mL acid mixture (HNO_3:H_2SO_4 7:3, v/v). About 500 μL of BrCl was later added to each sample and kept for 12 h to allow the conversion of Hg to Hg(II). Then, 5 mL of a 20 M sodium hydroxide (NaOH) solution were slowly added to each digest to ensure that the acid concentration was <20%. Finally, the digests were diluted to 1—3 ng mL^{-1} of Hg using Milli-Q water (18.2MΩ cm). Certified reference material (TORT-2, Lobster Hepatopancreas) was prepared in the same

110   way as the fish samples. The THg recovery of TORT-2 was in the range of 94—109% (n=6). A

111   mercury isotope analysis was based on a sample-standard bracketing method validated by Yin et

112   al. (2010b). The bracketing standard solutions (NIST SRM 3133) in a 10% acid solution

113   (HNO_3:H_2SO_4 = 7:3, v/v) were adjusted to within 10% of the THg concentration in the fish digests.

114   Mercury isotope compositions are reported in terms of per mil deviations from the NIST SRM

115   3133 Hg standard and expressed in delta notation (Blum and Bergquist, 2007):

$$\delta^{xxx}Hg(‰) = \{(^{xxx}Hg/^{198}Hg_{sample})/(^{xxx}Hg/^{198}Hg_{NIST\ 3133}) - 1\} \times 1000 \qquad (1)$$

116

117   and xxx represent the mass of Hg isotopes between 199 and 202. Hg-MIF is reported in DxxxHg

118   notation (deviation from mass dependency in units of permil,‰) using the following formulas

119   (Blum and Bergquist, 2007):

$$\Delta^{199}Hg \approx \delta^{199}Hg - (\delta^{202}Hg * 0.2520) \qquad (2)$$

$$\Delta^{201}Hg \approx \delta^{201}Hg - (\delta^{202}Hg * 0.7520) \qquad (3)$$

120

121   Replicate digests were prepared for each fish sample (n = 2) and standard reference material

122   (TORT-2) (n = 6). The UM-Almaden standard solution was measured once in every 10 samples.

123   Data uncertainties in this study corresponded to the larger value of the measurement uncertainty

124   of either the replicate fish digests or UMAlmaden. Measurements of UM-Almaden ($\delta^{202}Hg$: —

125   0.49 ± 0.11‰; $\Delta^{199}Hg$: —0.05 ± 0.08‰; $\Delta^{201}Hg$: —0.05 ± 0.06‰; 2σ, n = 11) were consistent

126   with previous data (Blum and Bergquist, 2007). As shown in Table 1, the TORT-2 ($\Delta^{202}Hg$: —

127   0.09 ± 0.12‰, $\Delta^{199}Hg$: —0.73 ± 0.08‰, $\Delta^{201}Hg$: —0.55 ± 0.08‰, 2 σ, n=6) was within the range

128   of errors of previous studies (Masbou et al., 2013; Tsui et al., 2012; Kwon et al., 2014).

RESULTS AND DISCUSSION

Differences in Hg isotope compositions between sediments and fish in the PRE

The Hg isotopic compositions of the 18 species of fish are summarized in Table S1 of Supporting Information. Various degrees of both δ^{202}Hg (—0.22 ± 0.10‰ to +0.38 ± 0.10‰) and Δ^{199}Hg (—0.05 ± 0.10‰ to +0.59 ± 0.30‰) (Fig. 2A and B) were observed   among different feeding guilds of fish, which may be interpreted as   having been caused by the mixing of isotopically distinct sources   and isotope fractionation during Hg biogeochemical cycling in sediments (or water column) and during trophic transfer to fish (Bergquist and Blum, 2007; Jackson et al., 2008; Das et al., 2009;   Gantner et al., 2009; Laffont et al., 2009, 2011; Gehrke et al.,   2011; Senn et al., 2010; Perrot et al., 2010, 2012; Kwon et al., 2012, 2013, 2014; Blum et al., 2013; Li et al., 2014).

In the PRE, Hg is released into the environment mainly ininorganic Hg (IHg) forms (Yin et al., 2015). Inorganic Hg is subsequently   converted to MeHg in deep anoxic water and sediments by sulfate- and iron-reducing bacteria (Fitzgerald et al., 2007; Kwon et al., 2014). An apparent increase in MeHg versus d13C was observed in the PRE fish, suggesting that the trophic transfer of   MeHgwas largely via the benthic pathway. In the PRE, high levels of MeHg in sediments (Shi et al., 2010) and high fractions of MeHg in seawater (~10%) have been reported (Fu et al., 2010), compared to   the much lower fractions of MeHg (~1%) in precipitation and river waters (Fu et al., 2010; Liu et al., 2012). This indicates that externalsources of MeHg (e.g., riverine and atmospheric inputs of MeHg) are generally limited in the PRE. The Hg isotopic compositions of the PRE sediments have been investigated and characterized to have relative low δ^{202}Hg (—1.92‰ to —0.68‰, n=27) and Δ^{199}Hg (—0.15 to +0.16‰, n=27) values (Yin et al., 2015). The

151   observation of the isotopic differences between fish and sediments is important for understanding

152   the biogeochemical cycling of Hg in the PRE. The positive offset in δ^{202}Hg between fish and

153   sediment in this study is well agreed with numerous recent studies. As no Hg-MDF has been

154   demonstrated to occur during the assimilation of Hg by fish (Kwon et al., 2012, 2013), we suggest

155   that fish mainly assimilate Hg with higher δ^{202}Hg values. d202Hg reported in this study are for

156   bulk fish Hg, which contains the dominant fraction of MeHg and minor IHg (Table S1). The IHg

157   in the PRE fish may represent the bioavailable IHg in sediments and water column, while MeHg

158   mainly comes from Hg methylation of the bioavailable IHg fractions. Bioavailable IHg species

159   have been reported as being characterized by higher δ^{202}Hg values (Yin et al., 2013a). The loss of

160   lighter Hg isotopes during Hg adsorption of sediment particles [containing thiol (Wiederhold et

161   al., 2010) and goethite (Jiska et al., 2012), Hg(II) photo-reduction (Bergquist and Blum, 2007;

162   Zheng and Hintelmann, 2009), microbial Hg(II) reduction (Kritee et al., 2013), and evasion

163   processes (Zheng et al., 2007) can shift the bioavailable IHg to higher δ^{202}Hg values. In sediments

164   and bottom water, MeHg is expected to have relative lower δ^{202}Hg than the IHg, because

165   preferential methylation of light Hg isotopes has been demonstrated during biotic and abiotic

166   methylation of bioavailable IHg (Rodríguez-Gonzalez et al., 2009; Jimenez-Moreno et al., 2013).

167   However, once transported to the surface water column via diffusion, advection and resuspension

168   processes, subsequent photo- and microbial-demethylation of Hg can shift the MeHg toward

169   higher δ^{202}Hg values (Bergquist and Blum, 2007; Kritee et al., 2013). Differences in water

170   conditions (e.g., depth and water clarity) may cause significant variations in the isotopic signatures

171   of IHg and MeHg in water column and fish among different regions (Blum et al., 2013). For

172   instance, Masbou et al. (2013) reported higher δ^{202}Hg in MeHg than in the IHg fraction, while

173   Jackson et al. (2008) demonstrated higher δ^{202}Hg in IHg than in the MeHg fraction. In this study,

174 negative correlations between fish δ^{202}Hg and THg (Fig. 3A, p < 0.05, ANOVA) were observed,

175 which contrasts with the findings reported in previous literature (Bergquist and Blum, 2007).

176 However, no clear correlation between δ^{202}Hg and FMeHg can be found (p > 0.3, ANOVA). Given

177 the fact that the fish collection represents diverse feeding habitats in different locations of the PRE,

178 it is still unclear whether the δ^{202}Hg variability represents the variability of MeHg with isotopically

179 distinct sources, or a mixing of IHg (with high δ^{202}Hg) and MeHg (with low δ^{202}Hg). Hence, more

180 studies are needed in the future to investigate the key processes involved in the subtropical estuary.

181 Compared to the PRE sediments, small positive Δ^{199}Hg values were observed for the fish in the

182 PRE (Fig. 2A). No clear correlations were observed between THg and Δ^{199}Hg (Fig. 3B, p > 0.10,

183 ANOVA), or between FMeHg and Δ^{199}Hg (p > 0.10, ANOVA). Insignificant Hg- MIF during

184 bioaccumulation and trophic transfer have been documented in prey-predator (e.g., fish-human,

185 fish-seal) (Laffont et al., 2009, 2011; Point et al., 2011; Perrot et al., 2012; Sherman et al., 2013;

186 Li et al., 2014) and plant studies (e.g., rice and aspen tree) (Demers et al., 2013; Yin et al., 2013b),

187 as well as fish feeding experiments (Kwon et al., 2012, 2013). The Hg-MIF has been understood

188 by the nuclear volume effect (NVE) and the magnetic isotope effect (MIE) (Schauble, 2007;

189 Buchachenko et al., 2007). In laboratory experiments, the NVEwas observed during several

190 processes [e.g., elemental Hg volatilization (Estrade et al., 2009), the non-photo reduction of Hg

191 species (Zheng and Hintelmann, 2010), and Hg-thiol complexation (Wiederhold et al., 2010)],

192 demonstrating Δ^{199}Hg / Δ^{201}Hg of ~1.6. These processes may not represent the Hg-MIF in the PRE

193 fish because the linear regression of Δ^{199}Hg and Δ^{201}Hg yielded a slope of 1.26 (Fig. 4, p < 0.05,

194 ANOVA), which is consistent with fish in other coastal regions (Gehrke et al., 2011; Senn et al.,

195 2010; Kwon et al., 2014). Laboratory experiments on the aqueous MeHg photo-degradation

196 induced by MIE showed Δ^{199}Hg / Δ^{201}Hg of ~1.3, which was in accordance with the Δ^{199}Hg /

197 Δ^{201}Hg observed in the PRE fish (Bergquist and Blum, 2007). Hence, it is thought that the Hg-

198 MIF is probably first generated by the MeHg photo-degradation prior to being transferred to fish.

199

200 **Using Hg-MIF to differentiate aquatic trophic structures**

201 Once methylated, MeHg can be released to the water column via diffusion, advection, and

202 resuspension, and subjected to photodegradation prior to being transferred to fish via food uptake

203 and bioaccumulation (Kwon et al., 2013). Therefore, Hg-MIF in fish can reveal important

204 information on the MeHg exposure pathways and characteristics of water columns (Bergquist and

205 Blum, 2007; Gantner et al., 2009; Gehrke et al., 2011; Senn et al., 2010; Blum et al., 2013; Sherman

206 and Blum, 2013; Kwon et al., 2014). In the present study, both demersal fish and herbivorous fish

207 showed lower THg and δ^{15}N values (Table 2 and Fig. 5). A possible explanation for this is the fact

208 that demersal fish mainly inhabit and feed on benthic organisms in bottom waters (close to

209 sediment interface), and herbivorous fish mainly live and feed on algae and seagrass in the photic

210 zone (Table S1). Large differences in Δ^{199}Hg values ($p < 0.05$, ANOVA) were observed between

211 demersal fish (mean: $+0.10 \pm 0.07$‰, σ, n$=$10) and herbivorous fish (mean: $+0.36 \pm 0.18$‰, σ,

212 n$=$10). The offset of Hg-MIF between the pelagic and benthic organisms was also reported in

213 several arctic lakes (Gantner et al., 2009) and in the North Pacific Subtropical Gyre (Blum et al.,

214 2013). The low Hg-MIF in demersal fish confirms that the source of MeHg in the PRE fish was

215 largely via the benthic pathways.We suggested that demersal fish are mainly exposed to a benthic

216 MeHg source that has not undergone much photochemical breakdown, while herbivorous fish are

217 more likely to represent MeHg that has undergone intensive photo-degradation in surface waters.

218 Carnivorous fish show intermediate mean Δ^{199}Hg value ($+0.24 \pm 0.09$‰, σ, n$=$20) between that

219   of demersal and herbivorous fish (Table 2). Carnivorous fish with the highest THg and δ^{15}N values

220   (Fig. 2) suggest that such fish prey upon herbivorous, demersal fish, and other marine species,

221   which will result in the intermediate Hg-MIF (Fig. 5). This further supports the hypothesis that the

222   Hg-MIF in biological samples is directly constrained by the isotopic signature of the assimilated

223   MeHg, rather than by in vivo mass-independent isotope fractionation (Blum et al., 2013; Kwon et

224   al., 2012, 2013).

225

Low Hg-MIF in the PRE fish

227   Fig. 4 shows differences in Hg-MIF among fish from different geographic areas. In comparison

228   with fish in the open ocean (Senn et al., 2010; Blum et al., 2013), much smaller Hg-MIF was

229   observed in fish in the PRE and other coastal areas (Gehrke et al., 2011; Kwon et al., 2014),

230   indicating that MeHg has undergone much less photodegradation before entering the coastal food

231   web. Differences in water circulation between the pelagic and coastal areas may be responsible for

232   the variability of fish Hg-MIF caused by the MeHg photo-degradation (Senn et al., 2010). The Hg-

233   MIF signatures in fish have been used to represent the degree of MeHg photodegradation in the

234   water column (Blum et al., 2013; Sherman et al., 2013; Kwon et al., 2014). In the PRE, a low rate

235   of MeHg photo-degradation is expected due to low water clarity in the PRE (generally < 1 m) and

236   to the riverine transport of large volumes of suspended particulate matter (Liu et al., 2012; Yin et

237   al., 2015). We estimated the percentage of MeHg photo-degradation based on the Δ^{199}Hg values

238   of the PRE fish. We calculated the expected relationship between Δ^{199}Hg and the fraction of Hg^{2+}

239   remaining in the aqueous system according to:

$$10^{3}*\ln[(10^{-3}\Delta^{199}Hg_{t} + 1)/(10^{-3}\Delta^{199}Hg_{i} + 1)] = S * \ln(1-f) \qquad (4)$$

240

241 Where f represents the fraction of MeHg that was photodemethylated; $\Delta^{199}Hg_i$ represents the initial

242 $\Delta^{199}Hg$ value ($\Delta^{199}Hg_i = 0$), and $\Delta^{199}Hg_t$ represents the $\Delta^{199}Hg$ value at a given time (here we use

243 the fish data). The slope (S) is calculated by plotting $10^3 * \ln[(10^{-3} \Delta^{199}Hg_t + 1)/(10^{-3} \Delta^{199}Hg_i + 1)]$

244 versus $\ln(1—f)$ for the relevant MeHg photo-degradation (Bergquist and Blum, 2007). For the 10

245 mg/L DOC photo-reductions of Hg^{2+} experiment, S $=$ $—7.82$. Finally, we estimated that less than

246 10% of MeHg is photo-degraded prior to entering the food web.

247

248 **CONCLUSION**

249 Coastal areas such as the PRE have received Hg inputs from natural and anthropogenic sources

250 (Yin et al., 2015). Methylation of Hg in deep anoxic waters and sediments contributes to the domi-

251 nant sources of Hg in aquatic ecosystems (Kwon et al., 2014). In the surface water column, MeHg

252 can be subjected to photo- degradation prior to being bioaccumulated into aquatic food webs;

253 hence, Hg-MIF can be subsequently coded in fish. The pre- sent study observed much lower Hg-

254 MIF in the PRE fish compared to other coastal and oceanic fish, indicating that much less MeHg

255 photo-degradation occurs in the PRE than in coastal and oceanic waters. The environmental risk

256 associated with MeHg in fish can increase due to the low efficiency of MeHg photo-degradation.

257 As a result, Hg-MIF in fish can be used to evaluate the process of MeHg accumulation. This study

258 documented for significant variability in Hg-MIF among herbivorous, demersal, and carnivorous

259 fish species, suggesting that different feeding guilds of fish may have incorpo- rated MeHg with

260 various degrees of photo-demethylation in the water column. Based on these results, we concluded

261 that Hg iso- topes (especially Hg-MIF) can be a powerful tool for revealing the exposure pathways

262 and geochemical behaviors of MeHg in coastal food webs.

269

270 Appendix A. Supplementary data

271 Supplementary data related to this article can be found at
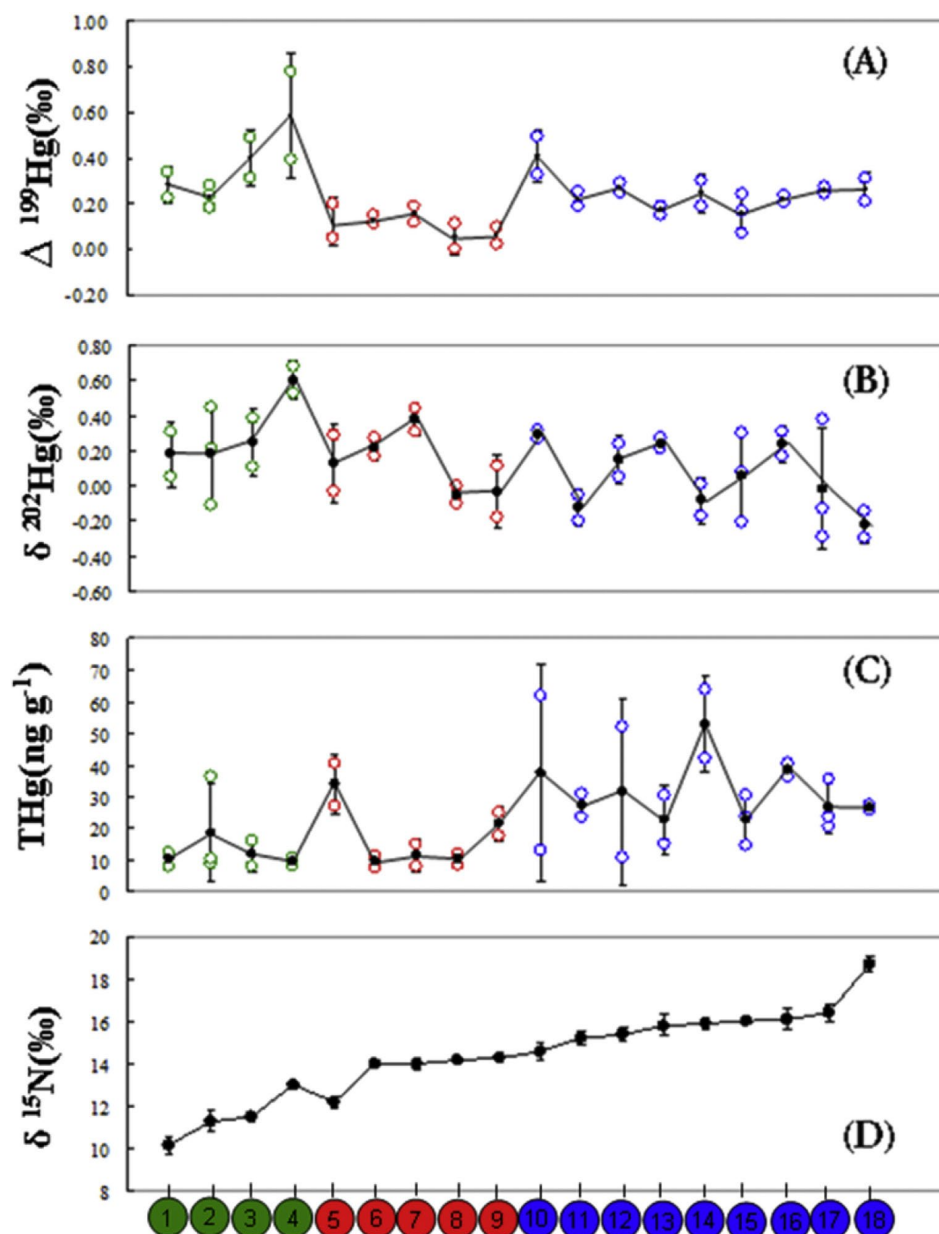
272 http://dx.doi.org/10.1016/j.chemosphere.2015.12.100.

273

LIST OF TABLES AND FIGURES

275

276   Fig. 1. Map showing the Pearl River Estuary (PRE), South China.

277

Fig. 2. δ^{202}Hg (A), Δ^{199}Hg (B), THg (C) and δ^{15}N (D) values in herbivorous [1. Flathead grey mullet (n = 2); 2.Western Pacific gizzard shad (n = 3); 3. Taiwanese mullet (n = 2) and 4. Silver pomfret (n = 2)], demersal [(5. Shortnose ponyfish (n = 2); 6. Large scale mullet (n = 2); 7. Mottled spinefoot (n = 2); 8. Speckled tonguesole (n = 2) and 9. Largescale tonguesole (n = 2)] and carnivorous fish [10. Belanger's croaker (n = 2); 11. Donkey croaker (n = 2); 12. Bartail flathead (n = 2); 13. Banded grouper (n = 2); 14. Devil stinger (n = 2); 15. Russell's Jewfish (n = 3); 16. Striped Catfish (n = 2); 17. Longtooth grouper (n = 3) and 18. Yellow Drum (n = 2)]. (For interpretation of the references to colour in this figure legend, the reader is referred to the web version of this article.)

287

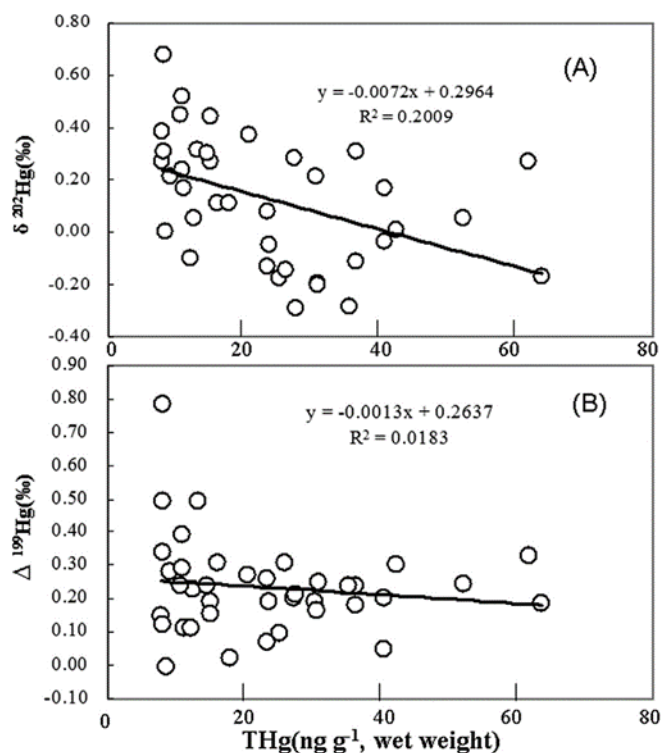Fig. 3. Correlations of THg to δ^{202}Hg (A) and Δ^{199}Hg (B) in the PRE fish.
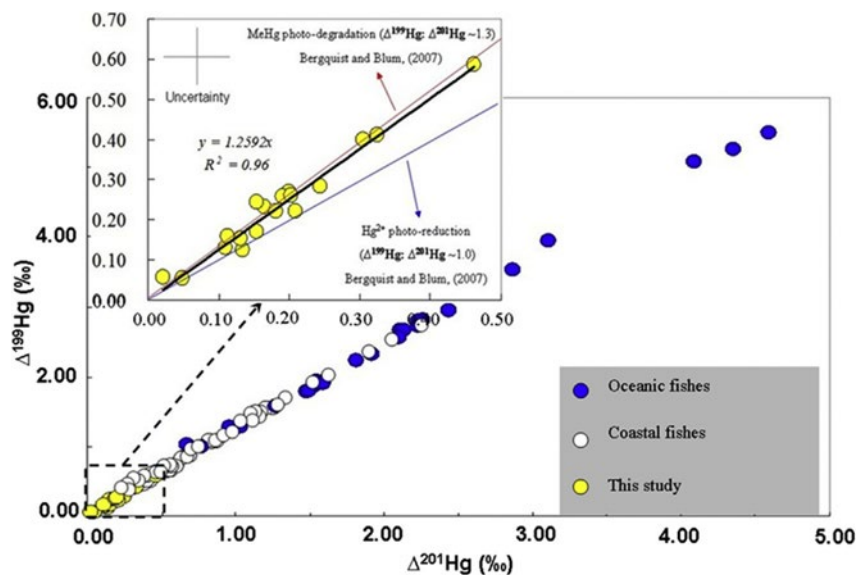
289

290

291

Fig. 4. Mass-independent fractionation of Hg in coastal and oceanic fish. Oceanic fishes were collected from Gulf of Mexico (Senn et al., 2010) and North Pacific Ocean (Blum et al., 2013); Coastal fishes were collected from Terrebonne Bay (Senn et al., 2010), San Francisco Estuary (Gehrke et al., 2011) and the Northeast coast estuaries (Kwon et al., 2014) of United States
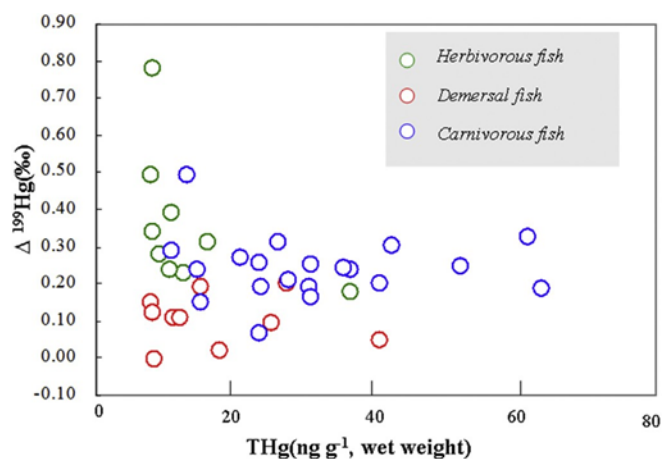
Fig. 5. Utilization of THg and Δ^{199}Hg to distinguish Hg sources in the PRE fish. ANOVA tests indicate statistic differences in Δ^{199}Hg values between herbivorous and demersal fish ($P < 0.05$), and statistically higher THg values for carnivorous fish than herbivorous and demersal fish ($P < 0.05$). Insignificant correlations can be observed with each group of fish, and the combined data ($P > 0.2$, ANOVA).

Table 1
Comparisons among the published Hg isotopic values of TORT-2.

δ^{202}Hg	2sd	Δ^{199}Hg	2sd	n	References
0.04	0.12	0.72	0.08	13	Tui et al. (2012)
0.10	n.a	0.79	n.a	1	Kwon et al. (2014)
−0.33	0.16	0.82	0.07	3	Masbou et al. (2013)
−0.09	0.12	0.73	0.08	6	This study

n.d. means not available.

Table 2
Fish species, δ^{15}N and δ^{13}C isotopes, Hg contents and bulk tissue Hg isotopic compositions in different fish groups of the PRE.

Fish groups	n	THg ng g^{-1}	σ ng g^{-1}	F_{MeHg} %	σ %	δ^{15}N ‰	σ ‰	δ^{202}Hg ‰	σ ‰	Δ^{199}Hg ‰	σ ‰	Δ^{201}Hg ‰	σ ‰
Herbivorous fish	9	75.8	33.3	94.1	5.8	11.48	1.00	0.29	0.25	0.36	0.18	0.30	0.16
Demersal fish	10	77.4	40.4	96.5	5.5	13.71	0.87	0.13	0.20	0.10	0.07	0.10	0.06
Carnivorous fish	20	208.2	314.3	98.6	7.4	16.03	1.05	0.06	0.23	0.24	0.09	0.19	0.08

REFERENCES

Bergquist, B.A., Blum, J.D., 2007. Mass-dependent and -independent fractionation of Hg isotopes by photoreduction in aquatic systems. Science 318, 417—420.

Blum, J.D., Berquist, B.A., 2007. Reporting of variations in the natural isotopic composition of mercury. Anal. Bioanal. Chem. 388, 353—359.

Blum, J.D., Popp, B.N., Drazen, J.C., et al., 2013. Methylmercury production below the mixed layer in the North Pacific Ocean. Nat. Geosci. 6, 879—884.

Blum, J.D., Sherman, L.S., Johnson, M.W., 2014. Mercury isotopes in earth and environmental sciences. Ann. Rev. Earth Planet. Sci. 42, 249—269.

Buchachenko, A.L., Ivanov, V.L., Roznyatovskii, V.A., et al., 2007. Magnetic isotope effect for mercury nuclei in photolysis of bis(p-trifluoromethylbenzyl) mercury. Dokl. Phys. Chem. 413, 39—41.

Das, R., Salters, V.J.M., Odom, A.L., 2009. A case for in vivo mass-independent fractionation of mercury isotopes in fish. Geochem. Geophys. Geosys. 10, Q11012.

Demers, J.D., Blum, J.D., Zak, D.R., 2013. Mercury isotopes in a forested ecosystem: implications for air-surface exchange dynamics and the global mercury cycle. Glob. Biogeochem. Cycle 27, 222—238.

Estrade, N., Carignan, J., Sonke, J.E., et al., 2009. Mercury isotope fractionation during liquid-vapor evaporation experiments. Geochim. Cosmochim. Acta 73, 2693—2711.

Fitzgerald, W., Lamborg, C., Hammerschmidt, C., 2007. Marine biogeochemical cycling of mercury. Chem. Rev. 107, 641—662.

Fu, X.W., Feng, X.B., Zhang, G., et al., 2010. Mercury in the marine boundary layer and seawater of the South China Sea: concentrations, sea/air flux, and impli- cation for land outflow, 1984—2012 J. Geophys. Res. 115 (D6).

Gantner, N., Hintelmann, H., Zheng, W., et al., 2009. Variations in stable isotope fractionation of Hg in food webs of arctic lakes. Environ. Sci. Technol. 43, 9148—9154.

Gehrke, G.E., Blum, J.D., Slotton, D.G., et al., 2011. Mercury isotopes link mercury in San Francisco Bay forage fish to surface sediments. Environ. Sci. Technol. 45, 1264—1270.

Hintelmann, H., 2012. Use of Stable Isotopes in Mercury Research. University of California Press, Berkeley.

Jackson, T.A., Whittle, D.M., Evans, M.S., et al., 2008. Evidence for mass-independent and mass-dependent fractionation of the stable isotopes of mercury by natural processes in aquatic ecosystems. Appl. Geochem 23, 547—571.

Jime,nez-Moreno, M., Perrot, V., Epov, V.N., Monperrus, M., Amouroux, D., 2013.

Chemical kinetic isotope fractionation of mercury during abiotic methylation of Hg(II) by methylcobalamin in aqueous chloride media. Chem. Geol. 336, 26e36. Jiska, M., Wiederhold, J., Bourdon, B., et al., 2012. Solution speciation controls mercury isotope fractionation of Hg(II) sorption to goethite. Environ. Sci.

Technol. 6, 6654—6662.

Kritee, K., Blum, J.D., Reinfelder, J.R., et al., 2013. Microbial stable isotope fraction- ation of mercury: a synthesis of present understanding and future directions. Chem. Geol. 336, 13—25.

Kwon, S.Y., Blum, J.D., Carvan, M.J., et al., 2012. Absence of stable isotope fraction- ation of methylmercury during trophic transfer in freshwater food webs. En- viron. Sci. Technol. 46, 7527—7534.

Kwon, S.Y., Blum, J.D., Chen, C.Y., et al., 2014. Mercury isotope study of sources and exposure pathways of methylmercury in estuarine food webs in the North- eastern US. Environ. Sci. Technol. 48, 10089—10097.

Kwon, S.Y., Blum, J.D., Chirby, M.A., et al., 2013. Application of mercury isotopes for tracing trophic transfer and internal distribution of mercury in marine fish feeding experiments. Environ. Toxicol. Chem. 32, 2322—2330.

Laffont, L., Sonke, J.E., Maurice, L., et al., 2009. Anomalous mercury isotopic com- positions of fish and human hair in the Bolivian Amazon. Environ. Sci. Technol. 43, 8985—8990.

Laffont, L., Sonke, J.E., Maurice, L., et al., 2011. Hg speciation and stable isotope signatures in human hair as a tracer for dietary and occupational exposure to mercury. Environ. Sci. Technol. 45, 9910—9916.

Li, M., Sherman, L.S., Blum, J.D., et al., 2014. Assessing sources of human methyl- mercury exposure using stable mercury isotopes. Environ. Sci. Technol. 48, 8800—8806.

Liu, J., Feng, X.B., Yin, R.S., et al., 2011. Mercury distributions and mercury isotope signatures in sediments of Dongjiang River, the Pearl River Delta. China. Chem. Geol. http://dx.doi.org/10.1016/j.chemgeo.2011.06.001.

Liu, J., Feng, X.B., Zhu, W., et al., 2012. Spatial distribution and speciation of mercury and methyl mercury in the surface water of East River (Dongjiang) tributary of Pearl River Delta, South China. Environ. Sci. Pollut. Res. 19, 105—112.

Masbou, J., Point, D., Sonke, J.E., 2013. Application of a selective extraction method for methylmercury compound specific stable isotope analysis (MeHg-CSIA) in biological materials. J. Anal. At. Spectrom. 28 (10), 1620—1628.

Pan, K., Chan, H., Tam, Y., et al., 2014. Low mercury levels in marine fish from estuarine and coastal environments in southern China. Environ. Pollut. 185, 250—257.

Perrot, V., Epov, V.N., Pastukhov, M.V., et al., 2010. Tracing sources and bio- accumulation of mercury in fish of Lake Baikal Angara River using Hg isotopic composition. Environ. Sci. Technol. 44, 8030—8037.

Perrot, V., Pastukhov, M.V., Epov, V.N., et al., 2012. Higher mass-independent isotope fractionation of methylmercury in the pelagic food web of Lake Baikal (Russia). Environ. Sci. Technol. 46, 5902—5911.

Point, D., Sonke, J.E., Day, R.D., et al., 2011. Methylmercury photodegradation influenced by sea- ice cover in Arctic marine ecosystems. Nat. Geosci. 4 (3), 188—194.

Rodríguez-Gonz,alez, P., Epov, V.N., Tessier, E., et al., 2009. Species-specific stable isotope fractionation of mercury during Hg(II) methylation by an anaerobic bacteria (Desulfobulbus propionicus) under dark conditions. Environ. Sci. Tech- nol. 43, 9183—9188.

Schauble, E.A., 2007. Role of nuclear volume in driving equilibrium stable isotope fractionation of mercury, thallium, and other very heavy elements. Geochim. Cosmochim. Acta 71, 2170—2189.

Senn, D.B., Chesney, E.J., Blum, J.D., et al., 2010. Stable isotope (N, C, Hg) study of methylmercury sources and trophic transfer in the northern Gulf of Mexico. Environ. Sci. Technol. 44, 1630—1637.

Sherman, L.S., Blum, J.D., 2013. Mercury stable isotopes in sediments and large- mouth bass from Florida lakes, USA. Sci. Total Environ. 448, 163—175.

Sherman, L.S., Blum, J.D., Franzblau, A., et al., 2013. New insight into biomarkers of human mercury exposure using naturally occurring mercury stable isotopes. Environ. Sci. Technol. 47, 3403—3409.

Shi, J., Ip, C.C.M., Zhang, G., et al., 2010. Mercury profiles in sediments of the Pearl River Estuary and the surrounding coastal area of South China. Environ. Pollut. 158, 1974—1979.

Tsui, M.T.K., Blum, J.D., Kwon, S.Y., et al., 2012. Sources and transfers of methyl- mercury in adjacent river and forest food webs. Environ. Sci. Technol. 46, 10957—10964.

Wiederhold, J.G., Daniel, K., Infante, I., et al., 2010. Equilibrium mercury isotope fractionation between dissolved Hg(II) species and thiol-bound Hg. Environ. Sci. Technol. 44, 4191—4197.

Yin, R., Feng, X., Shi, W., 2010a. Application of the stable-isotope system to the study of sources and fate of Hg in the environment: a review. Appl. Geochem. 25 (10), 1467—1477.

Yin, R.S., Feng, X.B., Foucher, D., et al., 2010b. High precision determination of mercury isotope ratios using online mercury vapor generation system coupled with multi-collector inductively coupled plasma-mass spectrometer. Chin. J. Anal. Chem. 38, 929—934.

Yin, R.S., Feng, X.B., Wang, J., et al., 2013a. Mercury isotope variations between bioavailable mercury fractions and total mercury in mercury contaminated soil in Wanshan mercury mine. S.W. China. Chem. Geol. 336, 80—86.

Yin, R.S., Feng, X.B., Meng, B., 2013b. Stable mercury isotope variation in rice plants (Oryza sativa L.) from the Wanshan mercury mining district, SW China. Environ. Sci. Technol. 47, 2238—2245.

Yin, R.S., Feng, X.B., Li, X.D., et al., 2014. Trends and advances in mercury stable isotope system as a geochemical tracer. Trends Environ. Anal. Chem. 2, 1—10.

Yin, R.S., Feng, X.B., Chen, B.W., et al., 2015. Identifying the sources and processes of mercury in subtropical estuarine and ocean sediments using Hg isotopic composition. Environ. Sci. Technol. 49, 1347—1355.

417 Zheng, W., Foucher, D., Hintelmann, H., 2007. Mercury isotope fractionation during volatilization
418 of Hg(0) from solution into the gas phase. J. Anal. At. Spectrom. 22, 1097—1104.

419 Zheng, W., Hintelmann, H., 2009. Mercury isotope fractionation during photore- duction in natural
420 water is controlled by its Hg/DOC ratio. Geochim. Cosmo- chim. Acta 73, 6704—6715.

421 Zheng, W., Hintelmann, H., 2010. Nuclear field shift effect in isotope fractionation of mercury
422 during abiotic reduction in the absence of light. J. Phys. Chem. A 114, 4238—4245.

423